Atmospheric Environment 155 (2017) 174–188

Contents lists available at ScienceDirect

Atmospheric Environment

journal homepage: www.elsevier.com/locate/atmosenv

Atmospheric emissivity with clear sky computed by E-Trans/HITRAN

Víctor M. Mendoza*, Elba E. Villanueva, René Garduño, Oscar Sánchez-Meneses

Centro de Ciencias de la Atmósfera, Universidad Nacional Autónoma de México, Ciudad de México, Mexico

HIGHLIGHTS

- A review of emissivity formulas from other authors, in terms of the vapour pressure and air temperature, is carried out.
- Cloudless atmosphere emissivity is computed using spectral calculator E-Trans with HITRAN database.
- Cloudless atmosphere emissivity is due to water vapour, CO_2, CH_4, N_2O and stratospheric O_3.
- Emissivity considers the vertical profiles of atmospheric temperature and pressure, and mixing ratio ones of these gases.
- Computed emissivity for the corresponding vapour pressures, agree well with those obtained by the reviewed authors.

ARTICLE INFO

Article history:
Received 23 May 2016
Received in revised form
13 December 2016
Accepted 26 January 2017
Available online 31 January 2017

Keywords:
Atmospheric emissivity
Greenhouse gases profiles
Vapour pressure
Semi-empirical parameterizations
Spectral calculator E-Trans/HITRAN

ABSTRACT

The vertical profiles of temperature and pressure from the International Standard Atmosphere, together with the mixing ratio profiles of the main greenhouse effect gases (GG), namely water vapour, CO_2, CH_4, N_2O and stratospheric O_3, are used to determine the downward emissivity of long wave radiation by cloudless atmosphere, by means of the spectral calculator E-Trans with the HITRAN (**hi**gh-resolution **tran**smission) database. We make a review of emissivity parameterizations, reported by several authors, in terms of the surface vapour pressure and surface air temperature. We compute vertically weighted averages of temperature and pressure, also parameterize the CH_4, N_2O and O_3 mixing ratio profiles, in order to adapt these variables as required by the E-Trans/HITRAN. Our results of emissivity for the corresponding vapour pressures agree well with those obtained by the reviewed authors. With this method, the emissivity can be computed at a regional scale and towards the future global warming, according to the IPCC temperature projections that will also increase the atmospheric humidity, from the emission scenarios of GG.

1. Introduction

The *emissivity* (ε) of a radiant surface is the fraction of radiation emitted by it (E), relative to that of the black body:

$$\varepsilon = \frac{E}{\sigma T^4} \tag{1}$$

where E is the energy flux (per area and time unit) emitted by the radiant surface at temperature T, σT^4 is the radiative flux of a black body at the same T, and σ is the Stefan-Boltzmann constant. Furthermore, the emitted fraction equals the absorbed, therefore emissivity and *absorptivity* have the same value if the radiative equilibrium is reached.

The downward atmospheric ε, which will be computed with (1), is necessary to determine the net long wave radiation in the surface-atmosphere interface, which is a very important component in climate models, especially to compute the greenhouse effect.

The main purpose of this paper is to use an alternative method to determine ε by means of the spectral calculator E-Trans (with the HITRAN database), which allows us to determine the combined ε of up to five mixed greenhouse effect gases (GG): water vapour, CO_2, CH_4, N_2O and O_3; assuming that each one of them homogeneously occupies a specific vertical space. We get ε as a function of the vapour pressure (e_a) and atmospheric temperature (T_a) both at surface level (denoted by the sub-index a), as is usual in (empirical or semi-empirical) formulas by other authors; although the first ones determine it as a function of only e_a. Emissivity ε should have

* Corresponding author. Centro de Ciencias de la Atmósfera, Universidad Nacional Autónoma de México (UNAM), Circuito Exterior, Ciudad Universitaria, 04510, Ciudad de México, Mexico.
E-mail address: victor@atmosfera.unam.mx (V.M. Mendoza).

http://dx.doi.org/10.1016/j.atmosenv.2017.01.048
1352-2310/

sub-index a, but we delete it to simplify the notation. All these formulas are compiled and compared in this work.

The paper is organized as follows: Section 2 includes the pioneer parameterizations of ε as a function of e_a; Section 3 deals with the Brutsaert's emissivity, introducing the *slab* concept and its dependence with atmospheric variables; Section 4 has the determination of water vapour *slab* emissivity (with a potential equation) from Brooks', Khun's and Staley and Jurica's tabulated data and the corresponding atmospheric emissivity; in Section 5, the vapour and CO_2 (by slab concept too) emissivities are combined, also corrected by their overlap. Section 6 presents the emissivity computed by E-Trans/HITRAN (from now on denoted E/H), with five subsections about the parameterization needed: 6.1 for vapour, 6.3 and 6.5 for CO_2 and O_3, respectively; the other GG (CH_4 and N_2O) in Subsection 6.4; as well as for the International Standard Atmosphere (ISA) in 6.2. Section 7 contains the results and discussion; finally, the conclusions appear in Section 8. The Appendix consists in the notation list.

2. Longwave emissivity by water vapour

Kondratyev (1965) and others set up that the net long wave radiation (I) at the surface-atmosphere interface depends on the vertical profiles of temperature and moisture of the atmosphere, and on the cloudiness. In this work, we will only deal with clear sky conditions (I_0), and the atmospheric *surface* variables mean their values at sea level (denoted by sub-index a). Budyko (1974) recorded some formulas to determine this net long wave radiation I_0.

On doing the radiative balance at the mentioned interface, we take as positive the flux from surface to atmosphere and the opposite as negative, therefore:

$$I_0 = \delta\left(\sigma T_S^4 - \varepsilon\sigma T_a^4\right) \tag{2}$$

where T_S is the temperature of the surface (sea or land) also called *skin* temperature and T_a is the surface air temperature; the surface emits $\delta\sigma T_S^4$ and absorbs, according to (1), $\delta E = \delta(\varepsilon\sigma T_a^4)$, where δ is the emissivity (or absorptivity) of the surface that depends on its nature, and ε is the emissivity of the atmosphere, which depends on the concentration of GG –mainly water vapour–, as well as on the atmospheric variables profile. The formulas presented in Sections 2, 3 and 4 refer to water vapour, and the other four GG are in the subsequent sections.

On climatic scales, T_S and T_a are very similar, so we can equal them, and (2) becomes:

$$I_0 = (1-\varepsilon)\delta\sigma T_a^4 \tag{3}$$

Among the first formulas of the kind (3) are the ones empirically obtained by Ångström (1916) and Brunt (1932), which are respectively

$$I_0 = \left(a_1 + b_1 10^{-c_1 e_a}\right)\delta\sigma {T_a}^4 \tag{4}$$

$$I_0 = (a_2 - b_2\sqrt{e_a})\delta\sigma {T_a}^4 \tag{5}$$

where T_a and the water vapour pressure e_a are measured ~2 m above the surface, and a_1, b_1, c_1, a_2 and b_2 are constants. The coefficient δ varies relatively little for different natural surfaces. Therefore, its average value, which equals to 0.95, is commonly used (Budyko, 1974); we will take this value in (4) and (5), and in the next formulas.

With climatologic data in Stockholm, Sweden, the Ångström constants take the values $a_1 = 0.21$, $b_1 = 0.26$ and $c_1 = 0.052$, when the e_a units are mb and those of I_0 are Wm^{-2}; these units will be used in the rest of this paper. On comparing (4) with (3), Ångström's emissivity is:

$$\varepsilon_A = 0.79 - 0.26 \times 10^{-0.052 e_a} \tag{6}$$

Based on measurements in Benson, southern England, Brunt's (1932) values of a_2 and b_2 are 0.45 and 0.065, respectively; therefore, according to (3) and (5), we have:

$$\varepsilon_{Br} = 0.55 + 0.065\sqrt{e_a} \tag{7}$$

According to Budyko's book (1974), using Kondratyev's (1951) results, Berliand and Berliand (1952) establish that I_0 satisfies Brunt's formula with the values $a_2 = 0.395$ and $b_2 = 0.0326$ i.e.:

$$I_0 = (0.395 - 0.0326\sqrt{e_a})\delta\sigma {T_a}^4 \tag{8}$$

So the emissivity of Berliand and Berliand is:

$$\varepsilon_{Bl} = 0.605 + 0.0326\sqrt{e_a} \tag{9}$$

Efimova (1961) finds that the Formula (8) agrees with the observed data during the International Geophysical Year (1957) for mid and high absolute humidity; at small humidity as in winter conditions on continental climate, (8) yields too high I_0 values. Therefore, Budyko (1974) proposes that formula of Berliand and Berliand (1952) should be modified as:

$$I_0 = (0.254 - 0.00495 e_a)\delta\sigma {T_a}^4 \tag{10}$$

Consequently, his emissivity is:

$$\varepsilon_{Bd} = 0.746 + 0.00495 e_a \tag{11}$$

Wales-Smith (1980) uses indirect monthly measures of I_0, in three stations of the United Kingdom: Kew (Surrey, southern England), Eskdalemuir (Dumfries, northern England) and Aldergrove (Northern Ireland), during the period 1964–70 for the first two and 1969–75 for the third one. With these measures, he establishes that the Brunt's formula with constants $\delta = 1$, $a_2 = 0.56$ and $b_2 = 0.08$ gives a good estimation of I_0. Therefore his formula is:

$$I_0 = (0.56 - 0.08\sqrt{e_a})\sigma {T_a}^4 \tag{12}$$

and for the emissivity:

$$\varepsilon_{WS} = 0.440 + 0.08\sqrt{e_a} \tag{13}$$

3. Brutsaert's emissivity

Brutsaert (1975) assumes an isotropic source function in a stratified atmosphere, therefore absorptivity and temperature depend on height only. This assumption allows to integrate the Schwarzschild's transfer equation over all directions and wavelengths, using the concept of *slab* emissivity, which was introduced by Brooks (1950), and consists in *reducing* the natural atmospheric column (denoted by subindex c) of height z to a laboratory slab (subindex s). This z is the vertical coordinate with its origin at *surface*, which is the topography over continent and the mean sea level (MSL) over ocean. He found that the column of optical thickness or water vapour content $a(z)$ radiates as a slab of *reduced* thickness $a/1.66$; so the emissivities are $\varepsilon_S(a/1.66)=\varepsilon_c(a)$. (Note that from Section 2 onwards and as a sub-index, a indicates the atmospheric variables referred at $z = 0$). By this way, Brutsaert arrives to the next formula:

$$E = \int_{a=0}^{a_T} \sigma T^4 \frac{\partial \varepsilon_c(1.66a)}{\partial a} da \tag{14}$$

where T is the temperature at z, the upper limit of the integral (14), a_T, is the *precipitable* water in the whole column, whose *top* (indicated by sub-index T) is at ~9 km; the lower limit of the integral (14) is the surface and corresponds to $a = 0$. To integrate it, the differential of a is scaled for the pressure effect:

$$da = \rho_w(z) \left[\frac{p(z)}{p_a}\right]^{1/2} dz \tag{15}$$

where $\rho_w(z)$ and $p(z)$ are the partial density of water vapour and the atmospheric pressure at z level, respectively; and p_a is the surface pressure.

In order to simplify the integral (14), Brutsaert assumes an exponential temperature profile:

$$T(z) = T_a \exp[-(\Gamma/T_a)z] \tag{16}$$

where $\Gamma = 6.5K\ km^{-1}$ is the lapse rate of the ISA, for the troposphere, above it the water vapour is negligible.

By using (16) and the equations of hydrostatic equilibrium and ideal gas, $p(z)$ can be determined with:

$$ln\frac{p(z)}{p_a} = -\frac{g}{R_d\Gamma}\left[\frac{\Gamma}{T_a}z + \frac{1}{2}\left(\frac{\Gamma}{T_a}z\right)^2 + \ldots\right] \tag{17}$$

where $g = 9.81\ ms^{-2}$ is the gravity acceleration and $R_d = 287.06\ J\ kg^{-1}K^{-1}$ is the gas constant of the dry air. For the ISA (also called by Brutsaert and other, *typical* value) $T_a = 288.15K$, at the tropopause $(\Gamma z/T_a) = 0.20$ and $(\Gamma z/T_a)^2/2 = 0.02$; in lower levels the ratio between these two values is greater, so in the series (17) we can keep the first term only. Therefore:

$$p(z) = p_a \exp[-(g/R_dT_a)z] \tag{18}$$

This profile corresponds to an isothermal atmosphere at temperature T_a.

For computing the partial density of vapour in (15), Brutsaert uses the next Yamamoto's (1949) formula, valid below 10 km:

$$e(z) = e_a \exp[-(k_w + \Gamma/T_a)z] \tag{19}$$

where $e(z)$ is the vapour pressure at z level and

$$k_w = 5.8 \times 10^3 K\left(\Gamma/{T_a}^2\right) - \Gamma/T_a + 0.055 km^{-1} \tag{19'}$$

By using (16), (19) and the ideal gas equation, we have

$$\rho_w(z) = \frac{0.622\ e_a}{R_dT_a}\exp(-k_wz) \tag{20}$$

Based on actual atmospheric measurements and on theoretical computations from other authors, Brutsaert finds for the emissivity of a slab of water vapour with CO_2, the following potential function:

$$\varepsilon_s(a) = A\ a^m \tag{21}$$

where the value of the parameters depends on the logarithmic range of a: in $0.01 < a < 1.0\ cm$, $m = 1/6$; whereas in $0.1 < a < 10.0\ cm$, $m = 1/8$; in both $A = 0.75$.Therefore:

$$E = \left[m\,A\left(\frac{0.622\ e_a}{k_2R_dT_a}\right)^m B(k_1/k_2, m)\right]\sigma\ {T_a}^4 \tag{22}$$

where $k_1 = 4\Gamma/T_a + k_2$, $k_2 = k_w + g/(2R_dT_a)$ and $B(\cdot\ ,\ \cdot)$ is the beta function.

We applied the Formula (20) that includes Yamamoto's exponential (19) on three places with different climates; using local values of Γ and T_a, the respective k_w value was computed and the vapour density profile was obtained and shown in Fig. 1. Table 1 synthetizes this information, giving also the data reference and indicating the curve in the the figure which in the three cases adjusts well to the observed data.

In order to determine E from (22), Brutsaert uses the Reitan's (1963) value $k_w = 0.44\ km^{-1}$ that is representative for the U.S. (and therefore with a T_a different of the global 288.15 K), the values $\Gamma/T_a = 0.0226\ km^{-1}$ for k_1 and $g/(R_dT_a) = 0.13\ km^{-1}$ for k_2, and for (21) he uses $A = 0.75$ and $m = 1/7$; therefore, Brutsaert's emissivity results:

$$\varepsilon_{Bs} = \frac{E}{\sigma\ T_a^4} = 1.24\left(\frac{e_a}{T_a}\right)^{1/7} \tag{23}$$

On deriving (23) from (14)–(22) it is not clear where Brutsaert incorporates the CO_2 emissivity as he mentions; rather, from (15),

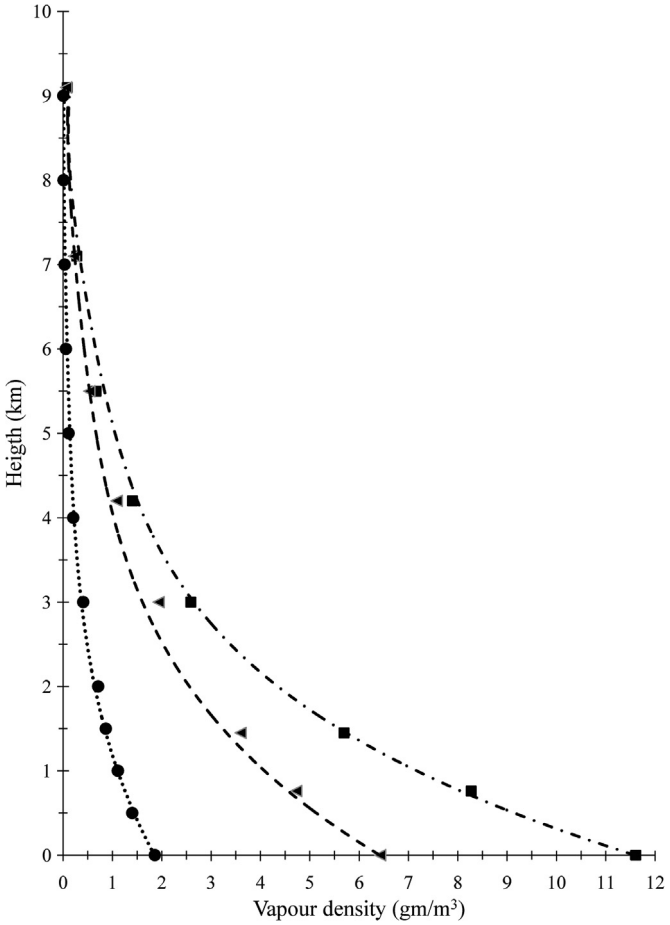

Fig. 1. Vapour partial density profiles computed with (20), adjusted to observed values (markers) in three places with different climates: Central Kentuky (squares), South California (triangles), both in US and from the NARR; and Terra Nova Bay (circles), Antartica, with data of Tomasi et al. (2004). More information about this figure appears in Table 1.

Table 1
Information about the data of the three water vapor density profiles shown in Fig. 1. Markers are observed data and curves are computed with (20).

Region	Climate	Reference	Γ ($K\ km^{-1}$)	$T_a(K)$	k_w (km^{-1})	Curve
Central Kentucky (37.8N, 85W)	Humid and temperate	NARR[a]	6.5	288.15	0.487	Dashed-dotted
South California (34N,116W)	Warm and dry	NARR[a]	6.5	298.0	0.458	Dashed
Terra Nova Bay, Antartica (74.7S, 164W)	Extremely dry and cold	Tomasi et al. (2004)	6.3	271.6	0.527	Dotted

[a] http//www.esrl.noaa.gov/psd/data/narr.

(19), (20) and (21), one would expect that emissivity (23) be only valid for vapour. In the next section we will deal with the vapour emissivity only and in the 6 with vapour and CO_2 together.

4. Other water vapour emissivities

Brooks (1950) plots slab emissivity $\varepsilon_s(a)$ for the water vapour, without CO_2, based on his own measurements (Brooks, 1941) and those of Robinson (1947, 1950). Brooks measured in laboratory the isothermal radiation for small values of $0.0001 \leq a < 0.003$ cm, whereas Robinson obtain field data for big $0.2 < a \leq 10.0$ cm. In the interval $0.003 \leq a \leq 0.2$ cm we interpolate ε_s between the Brooks' and Robinson's data, and with the physical hypothesis for $\varepsilon_s(a)$ to be a continuous and smooth function. With $A = 0.552$ and $m = 1/7$, we find that (21) reproduces well the Brooks' (1950) emissivity in $0.01 \leq a \leq 10.0$ cm.

Khun (1963) uses 211 nocturnal radiometersonde observations of infrared flux and tabulates $\varepsilon_s(a)$ values in the range $0.0001 < a < 3.0$ cm, which are well reproduced by (21) too, now with $A = 0.525$ and (again) $m = 1/7$.

Staley and Jurica (1970) report tables of experimental slab emissivities of the main bands of vapour, CO_2 and O_3, and of the overlap of the 15μ CO_2 band with the vapour rotational band, for −70, −40, −10 and 20 °C. For the vapour alone at −10 °C (closest to the mid troposphere temperature), (21) adjusts again, and very well, in $0.005 < a < 10.0$ cm, with $A = 0.604$ and $m = 1/6$.

With the ISA values of Γ and T_a, we get $k_w = 0.487\ km^{-1}$ from (19′). Now we use these three, together with the two of A and m values given in the last paragraphs, in (22) and (1) to obtain the emissivities ε using Brooks' (subindex Bk), Khun's (sub K), and Staley and Jurica's (sub SJ) data, which are:

$$\varepsilon_{Bk} = 0.91\left(\frac{e_a}{T_a}\right)^{1/7} \tag{24}$$

$$\varepsilon_K = 0.86\left(\frac{e_a}{T_a}\right)^{1/7} \tag{25}$$

and

$$\varepsilon_{SJ} = 1.10\left(\frac{e_a}{T_a}\right)^{1/6} \tag{26}$$

5. Combined emissivity of water vapour with CO_2

In order to determine the emissivity of vapour with CO_2, we use the slab values tabulated by Staley and Jurica (1970, their *total* in Table 1) at −10 °C. As we have said, the vapour slab emissivity can be expressed as:

$$\varepsilon_s(a) = 0.604a^{1/6} \tag{27}$$

where a is scaled by $[p(z)/p_a]^{1/2}$ and can be given as a function of z by integration of (15) from $z = 0$ until z; and using (16), (18) and (20), we have:

$$a(z) = a_0[1 - \exp(-k_2 z)] \tag{28}$$

where $a_0 = 0.622e_a/(k_2 R_d T_a)$ results in cm.

On its part, the emissivity of a CO_2 slab was adjusted by us as:

$$\varepsilon_s(b) = 0.0237 \ln(35b + 1) \tag{29}$$

where b is the amount of CO_2 given in centimeters at standard temperature and pressure (STP) conditions. The parametric Equation (29) adjusts very well to the experimental values of Staley and Jurica (1970, their Table 2), at −10 °C and in the wide range of values: $0.0001 \leq b \leq 1995cm$

According to Elsasser and Culbertson (1960), in a slab with the amount $db(z)$ of CO_2 the absorption by the 15μ band depends on the pressure, taken into account on scaling the slab by $[p(z)/p_a]^{0.88}$, i.e:

$$db(z) = \left(\frac{\rho(z) r_C}{\rho_C}\right)\left(\frac{p(z)}{p_a}\right)^{0.88} dz \tag{30}$$

where $\rho(z)$ is the air density and $\rho_C = 1.977\ kgm^{-3}$ is that of CO_2 at STP; r_C is the CO_2 mixing ratio assumed constant, Staley and Jurica (1972) use for it 500ppmm, which by the molecular weights of the CO_2 and the dry air is equivalent to 329.2 ppmv. We put this value in (30); nevertheless, in the next section we will use, according to Goody and Yung (1989), the greater value of 345ppmv.

Using (16) and (18) in (30), and integrating from $z = 0$, we get:

$$b(z) = b_0[1 - \exp(-k'_2 z)] \tag{31}$$

where $b_0 = p_a r_c/(k'_2 R_d T_a \rho_c)$ in cm and $k'_2 = 1.88g/(R_d T_a) - \Gamma/T_a = 0.20\ km^{-1}$.

The experimental values of Staley and Jurica (1970, their Table 5) for the emissivity correction due to the overlap of the vapour and CO_2 bands, mainly their rotational and 15μ bands, respectively, for −10 °C, can be well represented by the next parametric equation obtained by us, after an empirical adjustment (of two independent variables):

$$\Delta\varepsilon_s(a, b) = 0.008a^{0.42} \ln(35\, b + 1) \tag{32}$$

Therefore, according to Staley and Jurica (1970, 1972), the combined emissivity of vapour with CO_2 results:

$$\varepsilon_s(a, b) = \varepsilon_s(a) + \varepsilon_s(b) - \Delta\varepsilon_s(a, b) \tag{33}$$

On substituting (27)–(32) in (33), we obtain the atmospheric emissivity:

$$\varepsilon = \frac{1}{\sigma T_a^4}\int_0^{\varepsilon} \sigma T^4 d\varepsilon_s(a,b) = \underbrace{\int_0^{\varepsilon}\left(\frac{T}{T_a}\right)^4 d\varepsilon_s(a)}_{(i)} + \underbrace{\int_0^{\varepsilon}\left(\frac{T}{T_a}\right)^4 d\varepsilon_s(b)}_{(ii)} \times \underbrace{-\int_0^{\varepsilon}\left(\frac{T}{T_a}\right)^4 d\Delta\varepsilon_s(a,b)}_{(iii)} \approx \sum_{n=0}^{N}\left[\frac{e^{-(\Gamma/T_a)z_{n+1}} + e^{-(\Gamma/T_a)z_n}}{2}\right]^4 \{ \times [\varepsilon_s(a_{n+1}) - \varepsilon_s(a_n)] + [\varepsilon_s(b_{n+1}) - \varepsilon_s(b_n)] - [\Delta\varepsilon_s(a_{n+1}, b_{n+1}) - \Delta\varepsilon_s(a_n, b_n)]\} \quad (34)$$

where each integral (i, ii and iii) is a function of z only; by this way, we solve them with a finite summation of 1500 levels (N = 1500) and intervals $z_{n+1} - z_n = 10m$. The integration is carried out from $z = 0$, where $a = b = 0$, until $z = 15km$, at the tropopause; between these limits all the water and the 95% of CO_2 are included. At 15 km the temperature, given by (16) and used in (34), differs by no more than 5.2% from that of the ISA tropopause (216.65 K), which we will deal with later; in the summation the temperature has been replaced by its average between each two consecutive levels. By this way, our integration of (34) includes practically the totality of both gases and the use of the thermal profile (16), which facilitates the integration, does not yield a significant error.

6. Emissivity from the E-Trans/HITRAN

In this work we use an alternative method to determine the atmospheric emissivity, by means of the spectral calculator E-Trans with the HITRAN (**hi**gh-resolution **tran**smission) database. E-Trans/HITRAN is a software that allows us to compute the combined monochromatic transmittance of up to five mixed gases, each one of them homogeneous, in temperature, pressure and mixing ratio, and occupying vertical specific space. This software incorporates the respond function of the Fourier Transform spectrometers and utilizes the HITRAN database (version 2004; Rothman et al., 2005), which consists of a collection of spectroscopic parameters line-by-line, using a variety of computational codes, to simulate with the desired resolution the atmospheric transmission of the radiation (Rothman et al., 1987). The original purpose of this software was to detect atmospheric gases by their spectral signature and quantify them; now we propose a different use. For this objective, the gas nature, its thickness occupied, its mixing ratio (with respect to the dry air), the pressure and temperature should be specified in the E/H for each gas. For this, we introduce in the E/H five gases: water vapour, CO_2, CH_4, N_2O and O_3. The mixing ratio profile of the vapour is computed from its partial pressure given by (19); those of CO_2, CH_4 and N_2O are reproduced from the Goody and Yung's (1989) graph (Figure 1.5), which have the next features: the CO_2 mixing ratio is (constant) 345ppmv; and the ones of CH_4 and N_2O are 1.60 and 0.35 ppmv (respectively) at surface, both are almost constant along the troposphere, they diminish at the tropopause and the stratosphere, and ends with ~0.17ppmv and nearly zero above 70 and 60 km above MSL, respectively. The last gas introduced is the stratospheric O_3; its mixing ratio reaches a maximum from ~4.0 to 8.0 ppmv between ~27 and 35 km above MSL, and is negligible above 65 km and between the tropopause and the surface; we take a maximum of 6.34 ppmv at 27.2 km.

The E/H assumes that each gas is homogeneous in temperature and pressure; thus, to apply it to the atmospheric conditions that vary along the optical path, *equivalent* pressure and temperature should be introduced in order to approximate the transmitance of the inhomogeneous gas to that of the homogeneous. According to Smith (1969), these equivalent variables (indicated with the sub-index *e*; note that this symbol is also used for vapour pressure) are averages weighted with the gas content:

$$p_e = \frac{\int_0^U p du}{\int_0^U du} = \frac{\int_{H_L}^{H_U} p\, r\rho dz}{\int_{H_L}^{H_U} r\rho dz} \quad (35)$$

$$T_e = \frac{\int_0^U T du}{\int_0^U du} = \frac{\int_{H_L}^{H_U} T\, r\rho dz}{\int_{H_L}^{H_U} r\rho dz} \quad (36)$$

where U is the gas contained between the lower limit (H_L) and the upper one (H_U) of an atmospheric layer with a thickness H_U-H_L; and du is the gas contained in dz: $du = r\rho dz$, being r the mixing ratio of the gas. The E/H requires also a homogeneous mixing ratio for each gas; so, when it varies, we use its weighted average with the air density:

$$\bar{r} = \frac{\int_{H_L}^{H_U} r\rho dz}{\int_{H_L}^{H_U} \rho\, dz} \quad (37)$$

6.1. Water vapour

The strong vertical decay of the water vapour in the atmosphere is well described by (20), where $\rho_w(z) = r_w\rho$. Therefore, using (35), (36) and (37), with $H_L = 0$ we have:

$$p_{ew} = \left(\frac{k_w}{k_4}\right)\left(\frac{1-\exp[-k_4 H_U]}{1-\exp[-k_w H_U]}\right)p_a \quad (38)$$

$$T_{ew} = \left(\frac{k_w}{k_5}\right)\left(\frac{1-\exp[-k_5 H_U]}{1-\exp[-k_w H_U]}\right)T_a \quad (39)$$

$$\overline{r_w} = \left(\frac{k_3}{k_w}\right)\left(\frac{1-\exp[-k_w H_U]}{1-\exp[-k_3 H_U]}\right)\frac{0.622}{p_a}e_a \quad (40)$$

where $\bar{r}_w$ is the weighted average of vapour mixing ratio, $k_3 = g/R_d T_a - \Gamma/T_a$, $k_4 = k_w + g/R_d T_a$ and $k_5 = k_w + \Gamma/T_a$. Fig. 1, which shows $\rho_w(z)$, indicate that above 9 km the vapour is negligible, so we consider for it: $H_L = 0$ and $H_U = 9km$. By this way, with the ISA values for Γ, T_a and p_a, from (38) and (39), we get $p_{ew} = 821.3mb$ and $T_{ew} = 276.0K$. As an example to apply (40) and given that at T_a the saturation vapour pressure is ~17.0 mb, we take $e_a = 13mb$, which corresponds to 76% and is a representative value of the relative humidity (RH) of the actual surface atmosphere; so $\bar{r}_w = 2687.2$ppmm or 4321.0ppmv.

6.2. Standard atmosphere

In order to apply (35), (36) and (37) to CO_2, CH_4, N_2O and O_3, we use the pressure and temperature profiles from ISA, published by the International Standardization Organization (ISO, 1975). In this atmosphere, the pressure (P_a) and temperature (T_a) at MSL have the values just used in Subsection 6.1. The ISA is divided in eight layers, the first seven have linear profiles of temperature expressed as:

$$T(z) = T_k - \Gamma_k(z - z_k) \tag{41}$$

where $k = 0, 1, \ldots, 6$ identify each layer, z is the altitude above the MSL, T_k is the temperature at the base of layer ($z = z_k$) and Γ_k is the vertical constant lapse rate; (41) is not applicable to the eighth layer. Table 2 shows the features of the layers.

On using the ideal gas equation and assuming hydrostatic equilibrium and gravity constant, the corresponding pressure profile is:

$$p(z) = p_k\left[\frac{T_k - \Gamma_k(z - z_k)}{T_k}\right]^{\alpha_k} \quad for\ \ k<8 \tag{42}$$

where p_k is the pressure at $z = z_k$ and $\alpha_k = g/R_d\Gamma_k$ ($k = 0$ corresponds to sub-index a and $\Gamma_0 = \Gamma$). To use (42) in all layers of the ISA, we assume the tropopause and stratopause as nearly isothermal layers, with $\Gamma_1 = \Gamma_4 = -0.001K\ km^{-1}$.

6.3. Carbon dioxide

The atmospheric CO_2 is well mixed in almost the whole homosphere up to about 95 km (Goody and Yung, 1989), so its partial density is:

$$\rho_C(z) = r_C\rho(z) \tag{43}$$

where $r_C = 524.1$ppmm, equivalent to 345 ppmv; $\rho(z)$ from the ISA is determined by the ideal gas law:

$$\rho(z) = p(z)/[R_dT(z)] \tag{44}$$

The $\rho_C(z)$ is shown in Fig. 2, where it can be seen that above 40 km it is negligible, so we fixed $H_L = 0$ and $H_U = 45$ km for the CO_2 thickness. Using r_C in (35) and the hydrostatic equilibrium, its equivalent pressure is:

$$p_{eC} = \frac{p_a + p_H}{2} \tag{45}$$

where p_H is p at $z = H_U$. For its part, the equivalent temperature of CO_2 is:

$$\begin{aligned} T_{eC} = &\left(\frac{\alpha_0}{\alpha_0+1}\right)\left[\frac{p_a^{(\alpha_0+1)/\alpha_0} - p_1^{(\alpha_0+1)/\alpha_0}}{p_a^{1/\alpha_0}(p_a - p_H)}\right]T_a + \left(\frac{\alpha_1}{\alpha_1+1}\right) \\ &\times\left[\frac{p_1^{(\alpha_1+1)/\alpha_1} - p_2^{(\alpha_1+1)/\alpha_1}}{p_1^{1/\alpha_1}(p_a - p_H)}\right]T_1 + \left(\frac{\alpha_2}{\alpha_2+1}\right) \\ &\times\left[\frac{p_2^{(\alpha_2+1)/\alpha_2} - p_3^{(\alpha_2+1)/\alpha_2}}{p_2^{1/\alpha_2}(p_a - p_H)}\right]T_2 + \left(\frac{\alpha_3}{\alpha_3+1}\right) \\ &\times\left[\frac{p_3^{(\alpha_3+1)/\alpha_3} - p_H^{(\alpha_3+1)/\alpha_3}}{p_3^{1/\alpha_3}(p_a - p_H)}\right]T_3 \end{aligned} \tag{46}$$

Introducing ISA values in (45) and (46) we obtain $p_{eC} = 507mb$ and $T_{eC} = 250.1K$.

6.4. Methane and nitrous oxide

The vertical profiles of CH_4 (subindex M) and N_2O (subindex N) mixing ratio reported by Goody and Yung (1989) are well reproduced by means of the hyperbolic tangent function; by this way we have:

$$r_M(z) = 0.487\left[1 - 0.82\tanh\left(\sqrt{z} - \sqrt{z_I}\right)\right] \tag{47}$$

$$r_N(z) = 0.269\left[1 - 0.98\tanh\left(\sqrt{z} - \sqrt{z_I}\right)\right] \tag{48}$$

where z_I is the inflection level of the function, which in (47) is $36km$ and in (48) is $38km$.

At $z = 0$, $r_M = 0.886$ and $r_N = 0.532$ppmm, that are equivalent to 1.60 and 0.35ppmv, respectively. Fig. 3a and b, show the profiles up to 80 km given by (47) and (48), respectively. The corresponding partial densities are:

$$\rho_M(z) = r_M(z)\rho(z) \tag{49}$$

$$\rho_N(z) = r_N(z)\rho(z) \tag{50}$$

and appear in Fig. 3c and d, respectively; where we can see that above 40 km both gases are negligible; so we fix $H_L = 0$ and $H_U = 40$ km for both.

Due to the complexity of the hyperbolic tangent, the integrals (35), (36) and (37) are carried out numerically by the Simpson's trapezoidal rule. The results are for CH_4: $p_{eM} = 512.9mb$, $T_{eM} = 250.3K$ and $\bar{r}_M = 0.877$ppmm (1.583ppmv); and for N_2O: $p_{eN} = 512.2mb$, $T_{eN} = 250.3K$ and $\bar{r}_N = 0.528$ppmm (0.347ppmv).

6.5. Stratospheric ozone

Approximately 90% of the atmospheric ozone is located in a layer that starts between 10 and 17 km, and ends up to ~50 km; this is known as stratospheric ozone. The rest (~10%) is between the

Table 2
The eight layers of the ISA, their height intervals and the corresponding lapse rates and the temperature and pressure at the base of each layer.

k	Layer	Height z (km)	Γ_k ($K\ km^{-1}$)	Temperature at the layer base (K)	Pressure at the layer base (mb)
0	Troposphere	$0 < z \leq 11$	6.5	288.15	1013.25
1	Tropopause	$11 < z \leq 20$	0.0	216.65	226.32
2	Stratosphere	$20 < z \leq 32$	−1.0	216.65	54.75
3	Stratosphere	$32 < z \leq 47$	−2.8	228.65	8.68
4	Stratopause	$47 < z \leq 51$	0.0	270.65	1.11
5	Mesosphere	$51 < z \leq 72$	2.8	270.65	0.67
6	Mesosphere	$72 < z \leq 86$	2.0	214.65	0.04
7	Mesopause	$86 < z$	–	186.87	~0

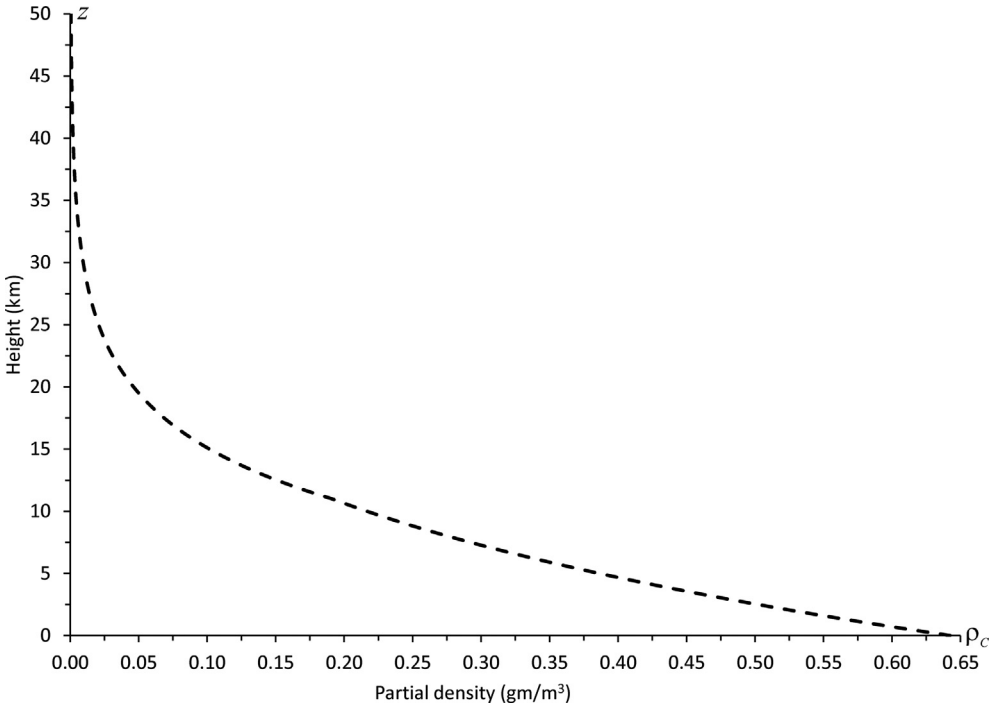

Fig. 2. Vertical profile of the CO_2 partial density computed with (43), according to Goody and Yung (1989), and the ISA.

surface and ~12.5 km, and is called tropospheric ozone (http://www.ozonelayer.noaa.gov/index.htm). Due to its abundance and by simplicity, we only take into account the stratospheric ozone; whose mixing ratio (r_O) reaches its maximum ($r_{O\max}$) at $z_{\max} \approx 30\ km$. In order to characterize its profile, we use the Gaussian formula:

$$r_O(z) = r_{O\max} \exp\left[-\gamma (z - z_{\max})^2 \right] \tag{51}$$

where $\gamma = 1.25 \times 10^{-2} km^{-2}$ is related to L, that is the *characteristic* width of the Gaussian curve; therefore, we assume that the *total* ozone mass is contained within the thickness $L = H_U - H_L$, where $H_L = z_{\max} - L/2$ and $H_U = z_{\max} + L/2$, and its amount per unit are is:

$$m_O = \int_{H_L}^{H_U} \rho_O(z) dz \tag{52}$$

where:

$$\rho_O(z) = r_O(z)\rho(z) \tag{53}$$

In order to solve the integral (52), we use the pressure profile of an isothermal atmosphere at temperature $\overline{T}$, instead of that in (42) from the ISA; therefore, according to (18):

$$p(z) = p_a \exp\left[-(g/R_d\overline{T})z \right] \tag{54}$$

where $\overline{T}$ is taken as 240 K, which is a simple average of the homosphere profile (until ~75 km) according to ISA. On comparing in semi-log scale, this profile (54) with that of the ISA (42), we find that both agree very well up to 75 km (figure not included in paper).

Using the state equation for the air, (51) and (54) in (53), we find:

$$\rho_O(z) = \frac{r_{O\max} p_a}{R_d \overline{T}} \exp\left[-\left(a' z^2 + 2b' z + c' \right) \right] \tag{55}$$

where $a' = \gamma$, $b' = g/2R_d\overline{T} - \gamma\, z_{\max}$ and $c = \gamma\, z_{\max}^2$. The profile of $\rho_O(z)$ has its maximum in z_0, which is also the mid height of the ozone layer, and differs from $z_{\max}$ because $r_O(z)$ is multiplied by the decaying function $\rho(z)$ to get $\rho_O(z)$ from (53). The value of z_0 can be determined by the equation:

$$\frac{d\rho_O(z)}{dz} = 0 \tag{56}$$

From which we find

$$z_0 = -b'/a' = z_{\max} - \frac{g}{2\gamma R_d \overline{T}} \tag{57}$$

In terms of z_0 we have

$$\rho_O(z) = \rho_{O\max} \exp\left[-a'\left(z^2 - z_0^2 \right) - 2b'(z - z_0) \right] \tag{58}$$

where $\rho_{O\max} = \rho_O(z_0)$. The value of this function decays to (*Euler number*)$^{-1}$ of its maximum in $z = z_0 \pm L/2$, i. e. where $a'(z^2 - z_0^2) + 2b'(z - z_0) = 1$, so $L = 2\sqrt{z_0^2 - c_0/\gamma}$, where $c_0 = -(a' z_0^2 + 2b' z_0 + 1)$.

By using (55) in (52), m_O can be expressed as:

$$m_O = \frac{r_{O\max} p_a}{2R_d T_0} \sqrt{\frac{\pi}{a'}} \exp\left(\frac{b'^2 - a'c'}{a'} \right) \left\{ erf\left[\sqrt{a'}\,(z_0 + L/2) + b' \Big/ \sqrt{a'} \right] - erf\left[\sqrt{a'}\,(z_0 - L/2) + b' \Big/ \sqrt{a'} \right] \right\} \tag{59}$$

where

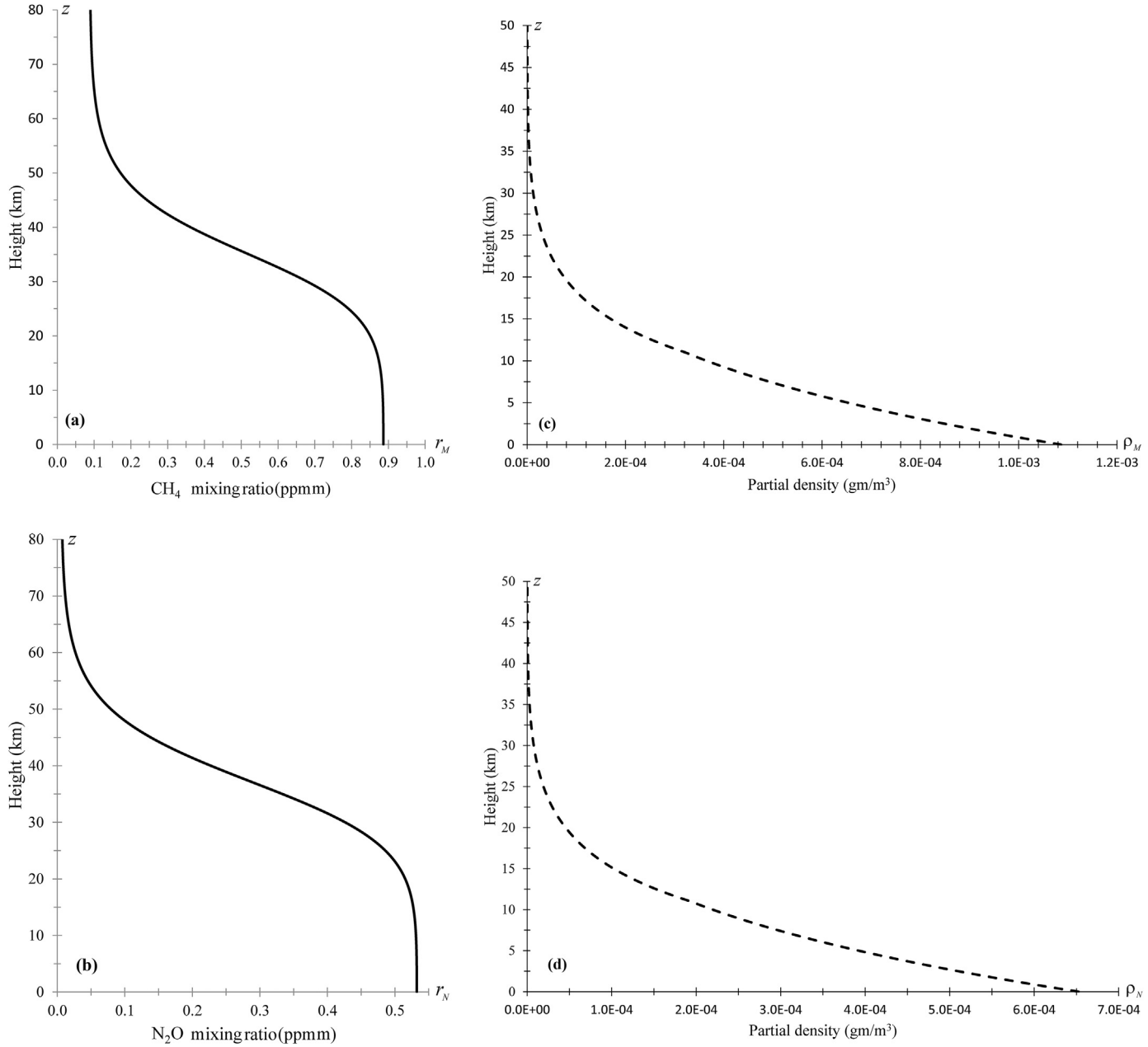

Fig. 3. Vertical profiles of the mixing ratio of: (a) CH_4 (subindex M) and (b) N_2O (subindex N); reported by Goody and Yung (1989). Both are adjusted by us through hyperbolic tangent functions (47) and (48), respectively; (c) and (d) are their corresponding partial densities (49) and (50).

$$erf(x) \equiv \frac{2}{\sqrt{\pi}} \int_0^x \exp\left(-t^2\right) dt$$

is the Gauss' error function.

Fig. 4 shows the vertical profile of the ozone *density number* (κ) in molecules cm^{-3}; part a) for February 22, 2007 at the station Table Mountain Test Facility at Boulder, CO, and part b) for December 18, 2007 at the station Fort Peck, MT, both measured by the night (http://www.ozonelayer.noaa.gov/index.htm). In both parts $\gamma = 1.25 \times 10^{-2} km^{-2}$, in a) $r_{O\max} = 8.2$ ppmm and $z_{\max} = 27.0km$, resulting in $m_O = 5.17 \times 10^{-3} kg\, m^{-2}$, equivalent to $6.49 \times 10^{22} molecules/m^2$ and to 241.6 Dobson units (DU), where 1DU = 0.001 cm, the $\kappa_{\max}$ is in $z_0 = 21{,}304$ m and $L = 17,888m$; in part b) $r_{O\max} = 10.5$ ppmm and $z_{\max} = 27.2km$, resulting $m_O = 6.43 \times 10^{-3} kg\, m^{-2}$ equivalent to $8.07 \times 10^{22} molecules/m^2$ and to 300.6 DU, the $\kappa_{\max}$ is in $z_0 = 21{,}504m$ and again $L = 17,888m$. Given that the standard column of O_3 amounts to 300DU, value also given by Staley and Jurica (1972), we take the Fort Peck profile as representative of the global atmosphere. In order to transform ρ to κ for any gas, we use $\kappa = \rho N_0 / M$, where N_0 is the Avogadro's number and M is the molecular weight of the gas.

The equivalent pressure is, according to (35):

$$p_{eO} = \frac{\int_{H_L}^{H_U} \rho_O(z) p(z) dz}{m_O} \tag{60}$$

where m_O is given by (52) and according to (53) and (54):

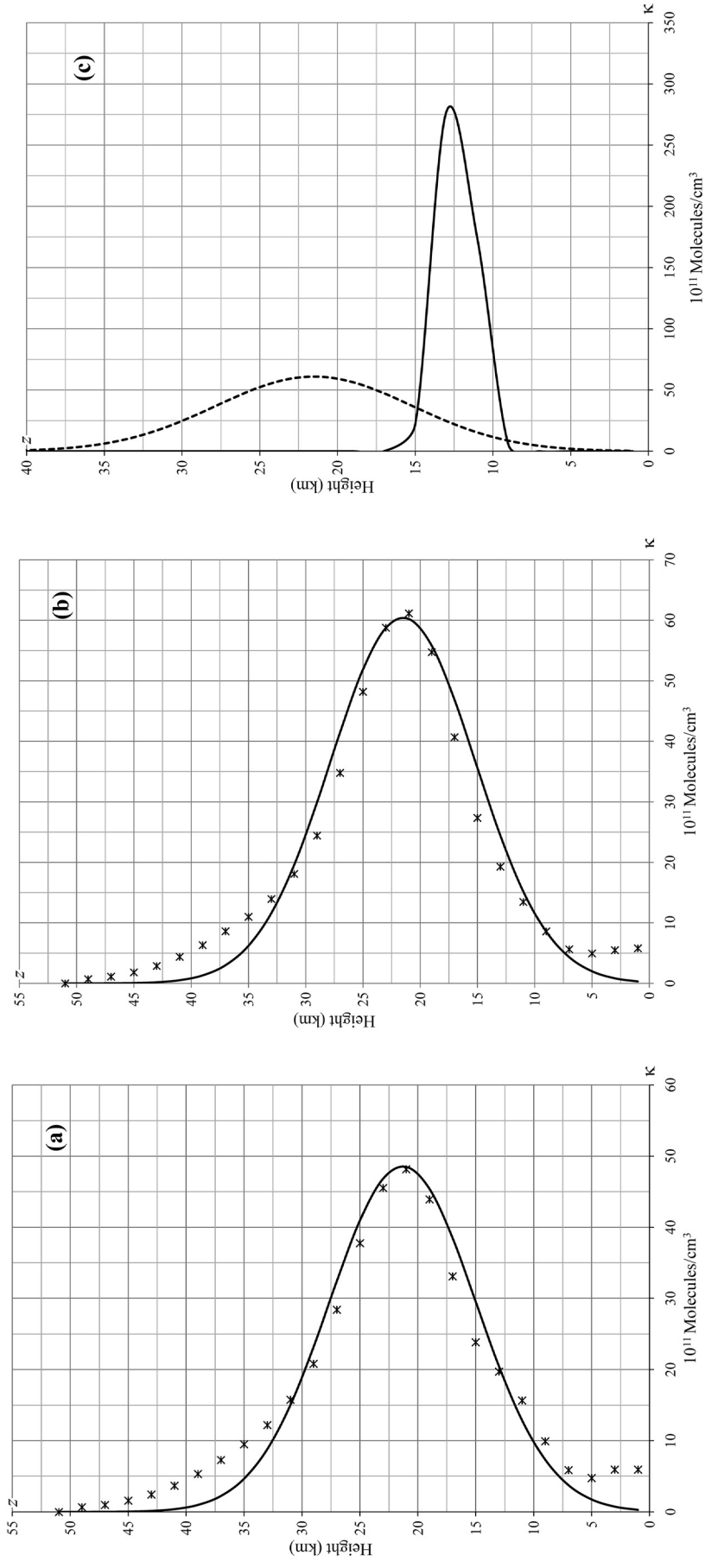

Fig. 4. Vertical profiles of the ozone concentration (κ): (a) and (b) are the observed data (crosses) for February 22, 2007 at the station Table Mountain, Boulder, CO, and for December 18, 2007 at the station Fort Peck, MT, respectively; the continuous lines are our adjustments. Part (c) shows the selected (original, Fig. 4b) profile of κ (dashed curve) and the corresponding shifted one towards the tropopause (continuous).

$$m_O \frac{p_{eO}}{p_a} = \frac{r_{O\max} p_a}{R_d \overline{T}} \int_{H_L}^{H_U} \exp\left[-\left(a' z^2 + 2b'' z + c' \right) \right] dz \tag{61}$$

The integrand in (61) is the same as (55), but with $b'' = b' + g/2R_d\overline{T} = g/R_d\overline{T} - \gamma\, z_{\max}$, instead of b'. On solving in (61) for p_{eO}, we get for the κ profiles of Fig. 4a and b the values 59.6 and 57.9 mb, respectively.

According to (37), (52), (53) and the state equation we have

$$\overline{r_O} = \frac{m_O}{\int_{H_L}^{H_U} \rho(z) dz} = \frac{R_d \overline{T}\, m_O}{\int_{H_L}^{H_U} p(z) dz} \tag{62}$$

On using (54) in (62) we obtain

$$\overline{r_O} = \frac{g}{p_a} m_O \left\{ \exp\left[-\frac{gH_L}{R_d \overline{T}} \right] - \exp\left[-\frac{gH_U}{R_d \overline{T}} \right] \right\}^{-1} \tag{63}$$

By this way, we have $\overline{r_O} = 3.16$ and 4.04 ppmm for Fig. 4a and b, respectively.

By consistency with the hypothesis given at the beginning of this sub-section, we assume that the equivalent temperature of the ozone layer is equal to that of the isothermal atmosphere, i. e. $T_{eO} = 240.0K$.

Given that the E/H does not resolve the transmitance for an atmospheric layer with an equivalent pressure less than 170 mb (127.5 Torr), we have "displaced" the ozone layer towards a lower level for the p_{eO} to be barely greater than 170 mb, but keeping m_O, under the hypothesis that its emissivity depends basically on the molecules amount (optical path) in the layer; possibly this pressure increase widens the emission band, but we assume this effect is negligible (M. Grutter, personal communication). We select the κ profile of Fig. 4b, whose maximum value is at $z_{\max} = 27,200\, m$; after applying the above mentioned shifting, the new profile has its maximum in $z'_{\max} = 12,500m$, and consequently $\gamma = 1.25 \times 10^{-2} km^{-2}$ changes to $\gamma' = 37.56 \times 10^{-2} km^{-2}$, keeping m_O, so that the lower tail of r_O enters the tropopause. Besides, now $z'_0 = 12,310\, m$, $\overline{r'_o} = 7.67$ppmm, $p'_{eO} = 176.7mb$ (132.5Torr) and $L' = 3,263.4\, m$. Fig. 4c shows the original profile of κ (dashed curve) and its shifted one towards the tropopause (continuous).

6.6. Transmittance from E-Trans/HITRAN

Table 3 compiles for the five GG the input E/H parameters: p_e, T_e, $\overline{r}$, as computed in the previous subsections, and the corresponding $H_U - H_L$. The $\overline{r}$ of the water vapour is determined for different values of e_a, although in the table only appears for 13 mb at 288.15 K, corresponding to RH = 76%. For the other gases their parameters have fixed values. With these values, the monochromatic transmittance is computed. The corresponding energy flux emitted by the vapour alone is plotted in Fig. 5a and the combination of the five GG is in Fig. 5b. Although these figures are shown up to 48μ, the emissivity was computed until 76μ.

Table 3
Input data of the five GG whose transmittance is computed by E/H. In the case of the vapour, data is only given for e_a = 13 mb, which for T_a = 288.15 K corresponds to saturation e_a of 17 mb, so RH = 76%.

Number	Gas	P_e		T_e (K)	$\overline{r}$		H_U - H_L (m)
		(mb)	(Torr)		(ppmm)	(ppmv)	
1	Vapour	821.3	616	276.0	2687.2	4321	9000
2	CO_2	507.6	380.7	250.1	524.1	345	45000
3	CH_4	512.9	384.7	250.3	0.877	1.587	40000
4	N_2O	512.2	384.1	250.3	0.528	0.347	40000
5	O_3	176.7	132.5	240.0	7.67	4.63	3263

7. Results and discussion

We can obtain from E/H, for each gas or for a homogenous mixture of gases, the monochromatic internal transmittance as a function of the wave number (in cm^{-1}), along the spectral interval from 131.1 to 5000 cm^{-1}; where a partition of 631 subintervals of 7.714 cm^{-1} every is selected. Additionally, we change the spectral independent variable to wavelength (λ), in this case the range is $2\mu \le \lambda \le 76\mu$. In order to get the emissivity (1), the energy flux E emitted downward by the atmospheric lower surface at temperature T_a, can be expressed in terms of transmittance as:

$$E = \int_0^\infty (1 - t_\lambda) B_\lambda(T_a) d\lambda \tag{64}$$

where t_λ is the monochromatic internal transmittance as a function of the wavelength and $B_\lambda(T_a)$ is the Planck's function at temperature T_a. Using (64) in (1), the atmospheric emissivity can be expressed by:

$$\varepsilon_{E/H} = 1 - \frac{1}{\sigma\, T_a^4} \int_0^\infty t_\lambda B_\lambda(T_a) d\lambda \approx 1 - \frac{1}{\sigma\, T_a^4} \int_2^{76} t_\lambda B_\lambda(T_a) d\lambda \tag{65}$$

As in former sections, sub-index a indicates atmospheric value at surface, here $\sigma {T_a}^4$ is the black body radiation at T_a. The approach to the finite integral in (65), may be justified because between 0 and 2μ the Planck's function is almost null and for λ > 76μ, $t_\lambda = 0$, because the vapour saturates the spectrum (as can be seen in Fig. 5), even for a relatively dry atmosphere in the surface (with surface values of relative humidity RH = 10% and temperature T_a). The integration in (65) is carried out using the Simpson's trapezoidal integration method with a partition of the corresponding 631 subintervals in λ.

Of course, in Fig. 5a and b, the emissivity ε is the shaded area divided by the total area below the Planck's curve. Table 4 shows the emissivity of the water vapour alone and that resulting when the other GG are successively included, and the percentage increase relative to the first.

The next three figures are semi-logarithmic for the variable e_a. Fig. 6, shows the emissivity of the vapour only; the dashed, dotted and dashed-dotted curves were obtained using (24), (25) and (26), respectively. The triangles and squares are explained two paragraphs below. The circles correspond to 12 different vapour pressure values used in (40), to compute its emissivity with the E/H and the equivalent pressure and temperature (38) and (39), respectively, with their ISA values. The continuous line adjusts well to the E/H results, so we get an equation similar to (24), (25) and (26):

$$\varepsilon_{E/H} = 1.22 \left(\frac{e_a}{T_a} \right)^{1/5.4} \tag{66}$$

These four equations for the interval $0 \le e_a \le 17mb$ are, in agreement with Brutsaert (1975), very insensitive to T_a; so for its typical value (288.15 K), he expresses it as suggested by Staley and Jurica (1972):

$$\varepsilon = C e_a^m \tag{67}$$

with $C = 0.427$ and $m = 0.185$ for $\varepsilon_{E/H}$ in (66). Fig. 6 shows also the curve (dashed-double dotted) of slab emissivity from Brutsaert,

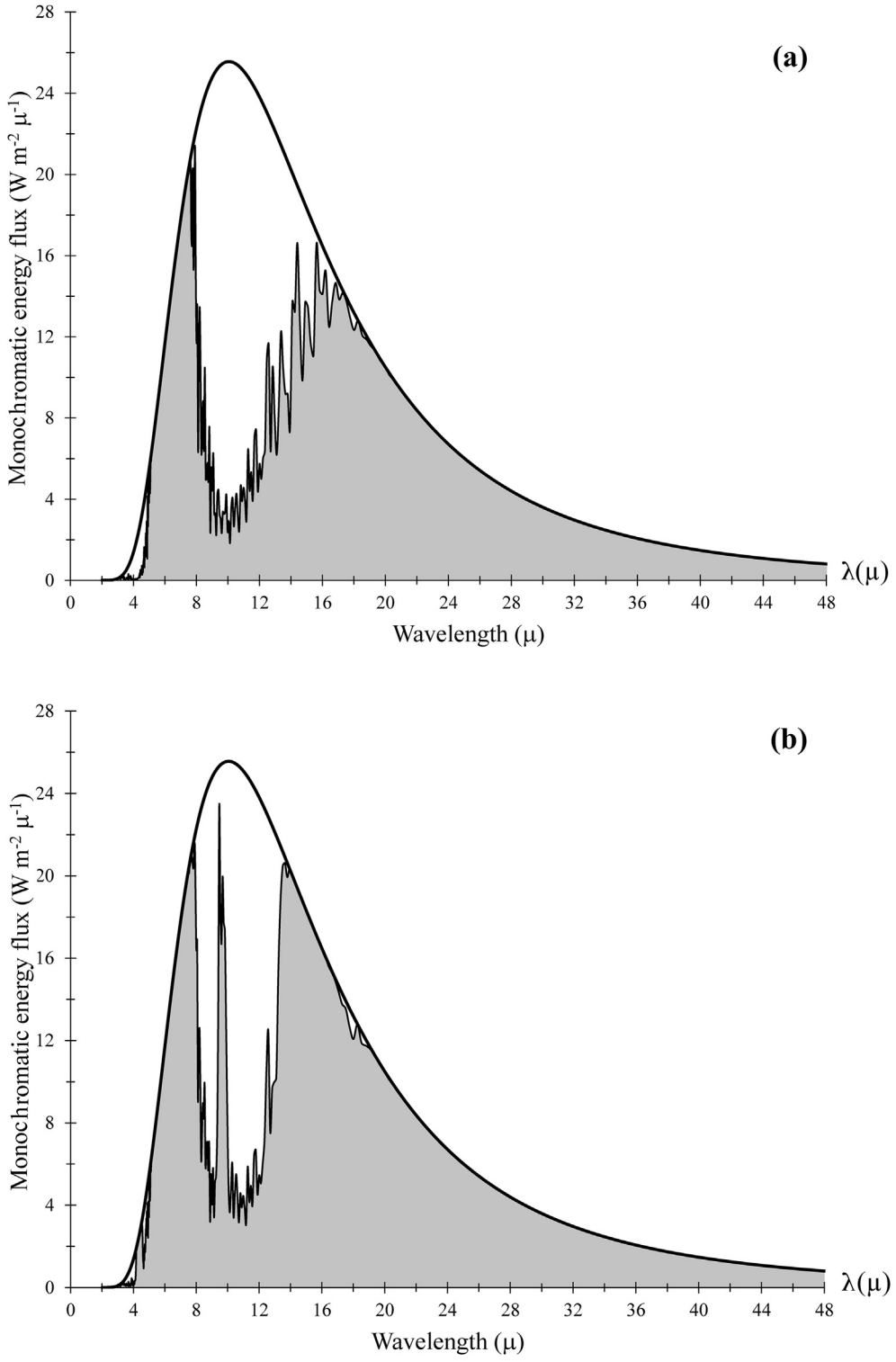

Fig. 5. Emission spectra (modulated by Planck's function) of water vapour alone (a) and of the five GG: water vapour, CO_2, CH_4, N_2O and stratospheric O_3 (b). Vertical axis is monochromatic energy flux emitted by the gas(es) as a function of wavelength. The shaded area is the complement of the transmittance computed by E/H.

which is almost parallel to that of E/H (continuous curve), but displaced upwards; probably due to his estimations of the vapour emissivity as it was applied to whole atmosphere, thus it results in an overestimation of the emissivity.

The curves of Brutsaert (obtained from 23), Brooks (24), Khun (25), and Staley and Jurica (26), differ among them only in the coefficient, which is 0.750, 0.552, 0.525 and 0.604, respectively; whilst the exponent of the first three is $m = 1/7$ and of the last one is 1/6. The SJ curve is the closest to the E/H one with (by analogy to the slab formulas) $m = 1/5.4$.

Staley and Jurica (1972) show (their Table 1) two sets of ε values as a function of e_a. The first set consists of nine values of the slab

Table 4
Emissivity computed by E/H for water vapour alone (first line) and that resulting when the other four GG are successively included, and the percentage increase with respect to the first.

Gas	Emissivity	Relative increase to the vapour (%)
H_2O	0.685	–
$H_2O + CO_2$	0.747	9.1
$H_2O + CO_2 + CH_4$	0.751	9.6
$H_2O + CO_2 + CH_4 + N_2O$	0.755	10.2
$H_2O + CO_2 + CH_4 + N_2O + O_3$	0.77	12.4

emissivity obtained from Jurica (1970), who used the laboratory transmissivity of high spectral resolution by Wyatt et al. (1962). The second set has only seven values obtained from the Staley and Jurica's (1972) slab emissivity and based on the Elsasser and Culbertson's (1960) data; with this we derived (27) in Section 5. The emissivity of the first set is between 0.03 and 0.06 greater than that of the second, because the Jurica's emissivity is ~0.02 greater than that of Staley and Jurica (1970), for an optical depth typical of the atmosphere. The first seven values of the first set are the triangles on Fig. 6, whilst the seven of the second set are the squares. Both sets of values and the curve obtained with (26) are the closest to those from E/H.

Table 5 shows, for the e_a nine values of Staley and Jurica (1972), the vapour emissivity (third column), this of CO_2 (fifth), their bands overlap (negative correction, seventh column) and the total of the three columns (ninth), with the first, second and third integrals, and their sum, all of (34); the corresponding values computed by the E/H appear in the second, fourth, sixth and eighth columns. On comparing our results with those of Staley and Jurica by (26), the ε for vapour from the first integral is consistently a bit less than theirs. For its part, the CO_2 emissivity from that second integral is only 0.01 greater than theirs. About the bands overlap from the third integral, it is very close, its absolute value increases together

Table 5
For the e_a nine values of Staley and Jurica (1972) (SJ), vapour emissivity (third column), this of CO_2 (fifth), their bands overlap (negative correction, seventh column) and the total of the three columns (nineth) are shown. The corresponding values computed by the E/H, with the first, second and third integrals, and their sum, all of (34), appear in the second, fourth, sixth and eighth columns.

e_a (mb)	Vapour		CO_2		Overlap		Total	
	E/H	S J	E/H	S J	E/H	S J	E/H	S J
0.237	0.34	0.38	0.20	0.19	−0.02	−0.02	0.52	0.55
0.706	0.40	0.44	0.20	0.19	−0.02	−0.03	0.58	0.60
1.83	0.47	0.51	0.20	0.19	−0.04	−0.04	0.63	0.66
4.22	0.54	0.57	0.20	0.19	−0.05	−0.06	0.69	0.70
6.14	0.58	0.6	0.20	0.19	−0.06	−0.07	0.72	0.72
8.73	0.61	0.65	0.20	0.19	−0.07	−0.09	0.74	0.75
15.8	0.68	0.71	0.20	0.19	−0.09	−0.11	0.79	0.79
31.9	0.76	0.82	0.20	0.19	−0.12	−0.14	0.84	0.87
51.7	0.82	0.89	0.20	0.19	−0.15	−0.17	0.87	0.91

with e_a and nevertheless the total also increase. Additionally, Staley and Jurica (1972) compute the emissivity due to the O_3 band (centered at ~9.5 μm), for a column of 0.30 cm (or 300 DU) representative of June and July in 30–35°N, resulting 0.05.

Fig. 7 has two curves: the dotted is the adjustment, in the interval $0.2 \le e_a \le 20mb$, to Staley and Jurica's (1972) results for the three gases vapour, CO_2 and O_3 (*total* column of their Table 1, the first seven values), represented by the triangles; the dashed curve corresponds to our results from the E/H for the five gases: vapour, CO_2, CH_4, N_2O and O_3 (12 values plotted by circles), adjusted in $0.2 \le e_a \le 17mb$. The dotted curve is computed by (67) with the parameters $C = 0.670$ and $m = 0.080$; the dashed curve is computed by the equation:

$$\varepsilon_{E/H} = \left(\frac{e_a}{T_a}\right)^{1/12} \tag{68}$$

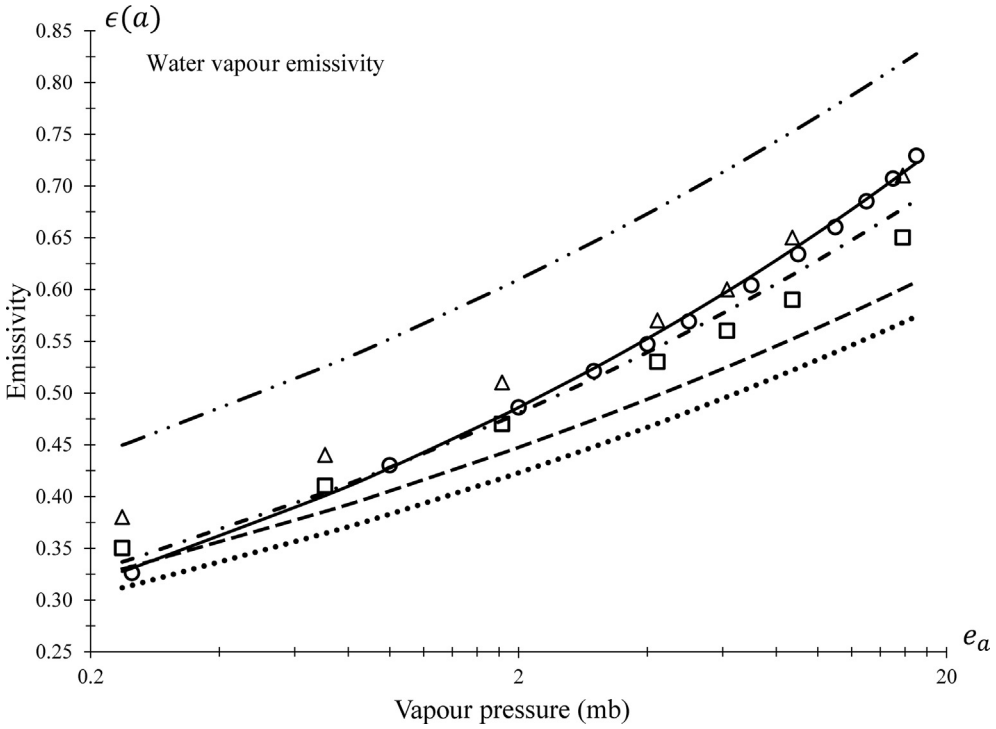

Fig. 6. Emissivity of the vapour only; the dashed, dotted and dash-dotted curves are obtained using (24), (25) and (26), from Brooks, Khun, and Staley and Jurica, respectively. The circles are the emissivity from the E/H, with 12 different vapour pressure values in (40); the continuous line is our adjustment to them. The triangles and squares are values from Staley and Jurica (1972). The dashed-double dotted curve is the slab emissivity from Brutsaert. For the parameters (A and m) values, refer to text.

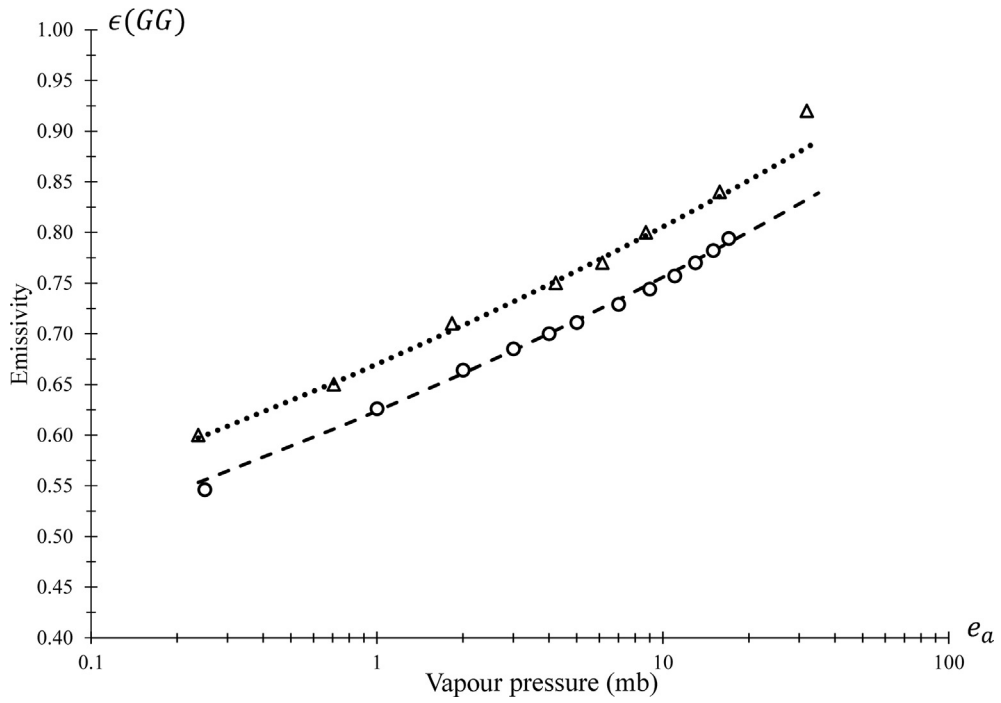

Fig. 7. The triangles are the first seven emissivities of the *total* column from Staley and Jurica's (1972, Table 1), for water vapour, CO_2 and O_3; dotted curve is their adjustment in. $0.2 \leq e_a \leq 20mb$ using (67), with $C = 0.670$ and $m = 0.080$. The circles are the 12 values from E/H for the five GG: water vapour, CO_2, CH_4, N_2O and O_3, adjusted by (68), with $C = 0.624$ and $m = 0.083$ (dashed curve), in $0.2 \leq e_a \leq 17mb$.

Using the typical value T_a, the (67) represents (68) with $C = 0.624$ and $m = 0.083$, this last value differs only a bit from the dotted curve exponent; therefore, this is the reason by which both curves are almost parallel. The exponent of (68) is significantly lower than in the cases that only have vapour, due to the addition of the other gases tends to saturate the spectrum and therefore the emissivity increases more slowly, i.e. it is less sensitive to the vapour pressure increment. In fact, the exponent (0.080) of the emissivity function of SJ, that includes CO_2 and O_3, in addition to the vapour, is almost equal to that of E/H (0.083); which means that the other gases (CH_4 and N_2O) contribute little to the slope of the emissivity. Nevertheless, the Staley and Jurica's coefficient C is significantly greater, possibly due to their emissivity is overvalued for not considering the decrease by the overlap of the 9.5μ O_3 band with the vapour band in the Simpson window.

Fig. 8 shows E/H emissivity (with circles) including the five gases, besides Brunt's (1932) curve and other 11 curves of its kind (7) with different coefficients and exponents, according to several authors. On comparing the curves, we find that Brunt's (1932), Goss and Brooks' (1956), and Berdahl-Martin's (1984) are the closest to the E/H one. The dispersion of those curves around this can be due to that the E/H one is computed as a global average, using temperature and pressure profiles from the ISA; on the other hand, the 12 curves are locally measured for different weather conditions; besides for their dispersion, it should be taken into account the difficulty to measure exactly the atmospheric long-wave radiation arriving to surface, greatly due to calibration errors of the pyrgeometer (Wang and Liang, 2009).

8. Conclusions

1. A literature review concerning various simplified methods to compute the atmospheric emissivity for clear sky conditions has been provided in this work. We find that since the pioneer works of Ångström (1916) and Brunt (1932), several authors have reported semi-empirical atmospheric emissivity parameterizations as a function of water vapour pressure at the surface level, and in certain cases also depending on the temperature at the surface. An important number of these parameterizations are similar in form to the Brunt equation, changing only the parameters value, due in part to the measurement site and greatly due to calibration errors of the pyrgeometer.
2. The purpose of the spectral calculator E/H is to identify gaseous components of the atmosphere with an ultra-high spectral resolution. In the manner in which we use it, i.e., in low spectral resolution (spectral bands), it represents adequately the downward long-wave atmospheric emissivity. The E/H is applied to a given gas, which is assumed to be homogeneous in temperature, pressure and mixing ratio; to use it in the non-homogeneous atmosphere; we have computed their equivalent temperature and pressure as averages weighted with the gas content (Smith, 1969); besides, when their mixing ratio is inhomogeneous we have used its average weighted with the air density. Using the E/H, we have computed the combined emissivity of the five atmospheric greenhouse gases: water vapour, CO_2, CH_2 N_2O and O_3 as a function of the water vapour pressure at the surface level. The result that we obtained agrees well with those of the other authors.
3. We, as Brutsaert (1975), have determined three parametric Equations (24)–(26) from laboratory data of *slab* emissivity for water vapour, reported by Brooks (1941) and Robinson (1947, 1950), of Khun (1963) and of Staley and Jurica (1970). We have also found a parametric Equation (66), using only water vapour in the E/H. All of these equations have the potential form of the Brusaert's kind (23); furthermore, their exponents have values in the relatively narrow range of $1/7 \leq m \leq 1/5.4$. This proves that the atmospheric emissivity can be well represented with only the vapour. On the other hand, when the CO_2 and O_3 are included, the exponent results smaller ($m \approx 1/12$) as computed by Staley and Jurica (1972) and by the E/H (that also includes

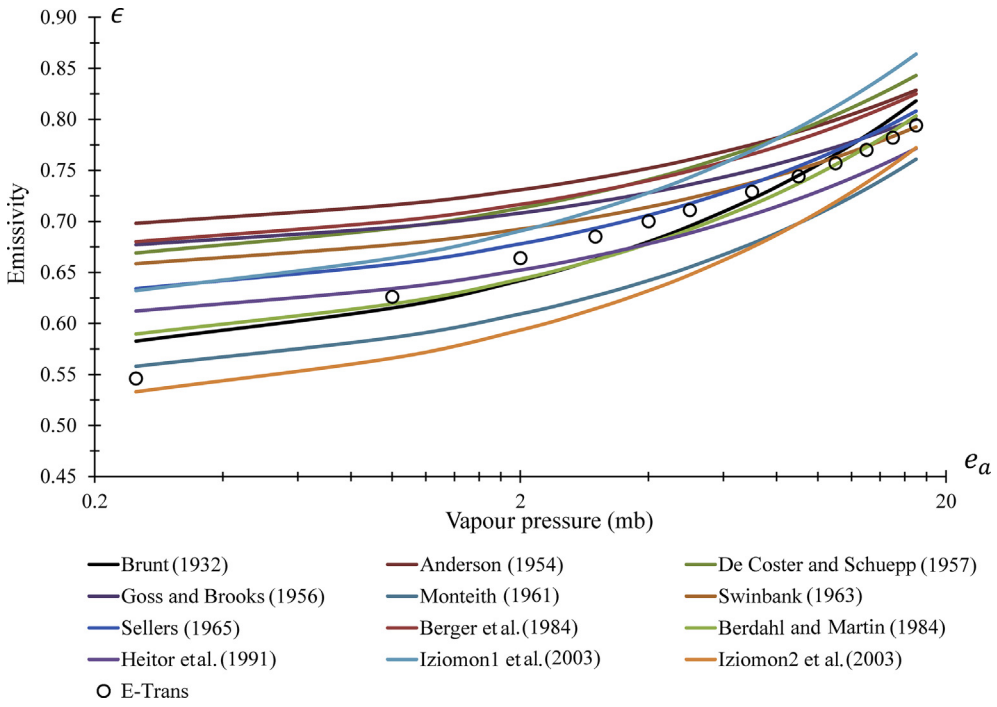

Fig. 8. E/H emissivity (denoted with circles) for the five GG: water vapour, CO_2, CH_4, N_2O and O_3; besides Brunt's (1932) curve given by (7) and other 11 curves of its kind with different coefficients and exponents, according to different authors. The Iziomon1 and Iziomon2 curves are from the same reference. (Anderson, 1954; Berger et al., 1984; De Coster and Schuepp, 1957; Heitor et al., 1991; Iziomon et al., 2003; Monteith, 1961; Sellers, 1965; Swinbank, 1963).

CH_4 and N_2O in 68). According to these results, this effect is due to that the addition of CO_2 and O_3 tends to saturate the spectrum and therefore the emissivity increases more slowly, i.e. it is less sensitive to the increase of the vapour pressure; besides, the inclusion of CH_4 and N_2O is even more insensitive.

4. Some authors experimentally determine the vapour emissivity from the *slab* concept; in a similar way, some authors determine the CO_2 emissivity. With the laboratory values of Staley and Jurica (1970), we have formulated a parametric Equation (33) for the combined slab emissivity of vapour with CO_2. The atmospheric emissivity (34) can be expressed as the sum of three integrals, ranging from the surface to 15 km altitude; the first integral corresponds to the vapour emissivity, the second one to that of CO_2 and the third one (which happens to be negative) to their bands overlap. The comparison between the emissivity computed with these integrals and the corresponding ones computed with the E/H, indicates that both results are acceptably similar.
5. The profiles of CH_4 and N_2O mixing ratio were parameterized by us with hyperbolic tangents. The O_3 concentration profile yields an equivalent pressure less than the minimum allowed (170 mb) by the E/H; in order to overcome this limitation, we have displaced this profile downwards in the atmosphere under two conditions: keeping the molecules amount in the column (optical path) and its equivalent pressure barely greater than 170 mb.
6. As a result of the present work, we propose the parametric Formula (68), as an additional one to those of Brunt (1932) and Brutsaert (1975), to estimate (with the ISA profiles) the global average of the atmospheric downward emissivity as a function of the surface vapour pressure (which is proportional to the relative humidity) and temperature there; in the validity interval around from 0.2 up to 20 mb (Figs. 7 and 8). According to conclusion 1, particularized to our ends, the rationale for this is that approximately 50% of surface downwards long-wave radiation flux comes from the lowest 100 m of the atmosphere under clear-sky conditions (Wang and Liang, 2009).

Acknowledgements

This work was partially supported by the Grant PAPIIT-UNAM, IN102415.We thank Michel Grutter for his valuable assistance about the basis and operation of the spectral calculator E-Trans/HITRAN, and Jorge Fujioka for clarifying us some mathematical functions.

Appendix. Notation

Γ	tropospheric lapse rate
g	gravity acceleration
R_d	gas constant of dry gas
GG	greenhouse effect gases
E/H	E-Trans/HITRAN
E	energy flux emitted (per area and time unit)
T	absolute temperature
T_a	atmospheric temperature at surface level
T_S	temperature of the surface (ocean and continent)
T_k	temperature at the base of k-th layer of ISA
p_k	pressure at the base of k-th layer of ISA
Γ_k	lapse rate in the k-th layer of ISA
σ	Stefan-Boltzmann constant
z	vertical level
e	vapour pressure
e_a	vapour pressure at surface level (2 m)
I	net long wave radiation at surface-atmosphere interface
I_0	net long wave radiation with clear sky conditions
ε	atmospheric emissivity
$A,\ m$	Coefficient and exponent, respectively, of a to compute ε_s
ε_A	Angstrom' s emissivity
ε_{Br}	Brunt's
ε_{Bl}	Berliand and Berliand's

ε_{Bd}	Budyko's
ε_{WS}	Wales-Smith's
ε_{Bk}	Brooks'
ε_{K}	Khun's
ε_{SJ}	Staley and Jurica's
ε_{Bs}	Brutsaert's
$\varepsilon_{E/H}$	E-Trans/HITRAN's
ε_s	slab emissivity
ε_c	column emissivity
$\Delta\varepsilon_s(a,b)$	emissivity correction due to overlap of vapour and CO_2
δ	surface emissivity
$a(z)$	slab vapour content between the surface and z
a_T	precipitable water
$b(z)$	slab CO_2 content between the surface and z
ρ	partial density of a gas
r	mixing ratio of a gas
$\overline{r}$	average of r weighted with the air density
p_e	equivalent pressure
T_e	equivalent temperature

For these five variables, the sub-indexes w, C, M, N and O, indicate vapour, CO_2, CH_4, N_2O and O_3, respectively

$p(z)$	atmospheric pressure at z
p_a	surface pressure
RH	relative humidity at surface
m_O	total ozone mass per unit area
λ	wave length
t_λ	monochromatic internal transmittance as a function of wave length
$B_\lambda(T)$	Planck's function at temperature T
$B(\cdot\ ,\ \cdot)$	beta function
H_L	lower limit of atmospheric vertical space occupied by each GG
H_U	upper limit of atmospheric vertical space occupied by each GG
U	gas content in the atmospheric vertical space (H_U-H_L)
L	characteristic width of O_3 Gaussian distribution
du	gas content in dz
ppmv	parts per million in volume
ppmm	parts per million in mass
STP	Standard Temperature and Pressure
MSL	mean sea level
IPCC	Intergovernmental Panel on Climate Change
ISA	International Standard Atmosphere
ISO	International Standardization Organization

References

Anderson, E.R., 1954. Energy budget studies, water loss investigation: Lake Hefner studies, technical report. U. S. Geol. Surv. Prof. Pap. 269, 71–119.

Ångström, A., 1916. Über die Gegenstrahlung der Atmosphäre. Meteorology Z.33 (12), 529–538.

Berdahl, P., Martin, M., 1984. Emissivity of clear skies. Sol. Energy 32, 663–664.

Berger, X., Buriot, D., Garnier, F., 1984. About the equivalent radiative temperature for clear skies. Sol. Energy 32, 725–733.

Berliand, M.E., Berliand, T.G., 1952. Determining the net long-wave radiation of the Earth with consideration of the effect of cloudiness. Izv. Akad. Nauk. SSSR Ser. Geofiz. 1.

Brooks, D.L., 1950. A tabular method for the computation of temperature change by infrared radiation in the free atmosphere. J. Meteorol. 7, 313–321.

Brooks, F.A., 1941. Observations of atmospheric radiation. Pap. Phys. Ocean. Meteor., Mass. Inst. Tech. Woods Hole Ocean. Instn. 8 (2), 23pp.

Brunt, D., 1932. Notes on radiation in the atmosphere. Quart. J. Roy. Meteorol. Soc. 58, 389–420.

Brutsaert, W.H., 1975. On a derivable formula for long-wave radiation from clear skies. Water Resour. Res. 11, 742–744. http://dx.doi.org/10.1029/WR011i005p00742.

Budyko, M.I., 1974. Climate and Life. Int. Geophys. Series, vol. 18. Academic Press, London, 508pp.

De Coster, M., Schuepp, W., 1957. Mesures de rayonnement effectif a Leopoldville. Acad. Roy. Sci. Colon., Bruss. Bull. Seances 3, 642–651.

Efimova, N.A., 1961. On methods of calculating monthly values of net long-wave radiation. Meteorol. Gidrol. 10, 28–33. MGA 13.9-523.

Elsasser, W.M., Culbertson, M.F., 1960. Atmospheric radiation tables. Meteor. Monogr. 4 (23), 1–43.

Goody, R.M., Yung, Y.L., 1989. Atmospheric Radiation. Theoretical Basis, second ed., xvi. Oxford University Press, New York. 519 pp.

Goss, J.R., Brooks, F.A., 1956. Constants for empirical expressions for downcoming atmospheric radiation under cloudless sky. J. Meteorol. 13, 482–488.

Heitor, A., Biga, A.J., Rosa, R., 1991. Thermal radiation components of the energy balance at the ground. Agric. For. Meteorol. 54, 29–48.

ISO, 1975. International Organization for Standardization, Standard Atmosphere. ISO, p. 2533, 1975.

Iziomon, M.G., Mayer, H., Matzarakis, A., 2003. Downward atmospheric irradiance under clear and cloudy skies: measurement and parameterization. J. Atmos. Sol. Terr. Phys. 65, 1107–1116.

Jurica, G.M., 1970. Radiative Flux Densities and Heating Rates in the Atmosphere Using Pressure and Temperature-dependent Emissivities. Ph. D. dissertation. University of Arizona.

Khun, P.M., 1963. Radiometersonde observations of infrared flux emissivity of water vapor. J. Appl. Met. 2, 368–378.

Kondratyev, K. Ya, 1951. On the approximate calculation of net long-wave radiation at the earth's surface. Inf. Sb. Leningr. Din. I Sel'skokhoziaistvennaia Meteorol. 1, 88–90. MGA 3:600.

Kondratyev, K. Ya, 1965. Radiative Heat Exchange in the Atmosphere. Pergamon Press, London, 411pp.

Monteith, J.L., 1961. An empirical method for estimating long-wave radiation exchanges in the British Isles. Quart. J. Roy. Meteorol. Soc. 87, 171–179.

Reitan, C., 1963. Surface dew point and water vapor aloft. J. Appl. Meteorol. 2, 776–779.

Robinson, G.D., 1947. Notes on the measurement and estimation of atmospheric radiation. Quart. J. Roy. Meteorol. Soc. 73, 127–150. http://dx.doi.org/10.1002/qj.49707331510.

Robinson, G.D., 1950. Notes on the measurement and estimation of atmospheric radiation-2. Quart. J. Roy. Meteorol. Soc. 76, 37–51. http://dx.doi.org/10.1002/qj.49707632705.

Rothman, L.S., Gamache, R.R., Goldman, A., Brown, L.R., Toth, R.A., Pickett, H.M., Poynter, R.L., Flaud, J.M., Camy-Peyret, C., Barbe, A., Husson, H., Rinsland, C.P., Smith, M.A.H., 1987. The HITRAN database: 1986 edition. Appl. Opt. 26, 4058–4097.

Rothman, L.S., Jacquemart, D., Barbe, A., Chris Benner, C., Birk, M., Brown, L.R., Carleer, M.R., Chackerian Jr., C., Chanse, K., Coudert, L.H., Dana, V., Devi, V.M., Flaud, J.-M., Gamache, R.R., Goldman, A., Hartmann, J.-M., Jucks, K.W., Maki, A.G., Mandin, J.-Y., Massie, S.T., Orphal, J., Perrin, A., Rinsland, C.P., Smith, M.A.H., Tennyson, J., Tolchenov, R.N., Toth, R.A., van der Auwera, J., Varanesi, P., Wagner, G., 2005. The HITRAN 2004 molecular spectroscopic data base. JQSRT 96, 139–204.

Sellers, W.D., 1965. Physical Climatology. Univ. of Chicago Press., Chicago. Ill. 272pp.

Smith, W.L., 1969. A Polynomial Representation of Carbon Dioxide and Water Vapor Transmission, vol. 47. E.S. S. A. Tech. Report. Rep. N. E. S. C.

Staley, D.O., Jurica, G.M., 1970. Flux emissivity tables for water vapor, carbon dioxide and ozone. J. Appl. Meteor. 9, 365–372.

Staley, D.O., Jurica, G.M., 1972. Effective atmospheric emissivity under clear skies. J. Appl. Meteor. 11, 349–356.

Swinbank, W.C., 1963. Long −wave radiation from clear skies. Quart. J. Roy. Meteorol. Soc. 89, 339–348.

Tomasi, C., Cacciari, A., Vitale, V., Lupi, A., Lanconelli, Ch., Pellegrini, A., Grigioni, P., 2004. Mean vertical profiles of temperature and absolute humidity from a 12 year radiosounding data set at Terra Nova bay (Antartica). Atmos. Res. 71, 139–169.

Wales-Smith, B.G., 1980. Estimates of net radiation for evaporation calculations. Hydrol. Sci. Bull. Des. Sci. Hydrol. 25 (3), 237–242, 9.

Wang, K., Liang, S., 2009. Global atmospheric downward longwave radiation over land surface under all-sky conditions from 1973 to 2008. J. Geophys. Res. 114, D19101. http://dx.doi.org/10.1029/2009JD011800.

Wyatt, P.J., Stull, V.R., Plass, G.N., 1962. The Infrared Absorption of Water Vapor. Final Rept., SSD-TDR-62-127, II. Aeronautronic Div., Ford Motor Co., 249pp.

Yamamoto, G., 1949. Average vertical distribution of water vapour in the atmosphere. Sci. Rep. Tohoku Univ. Ser. 5 (1), 76–79.